Study of competitive adsorption of acid dyes on magnetic quaternary chitosan salt

Conglu Zhang, Xiaohong Hou, Ning Liang, Yueyue Ding and Xiaomin Hu

ABSTRACT

Magnetic quaternary chitosan salt CS/EPTAC/Fe_3O_4 was used for the removal of acid red 1 (AR1), xylenol orange (XO) and alizarin red (AR) in single, binary and ternary systems. In the single system, the maximal adsorption capacity was 781.55 for AR1, 537.40 for XO and 992.61 mg g^{-1} for AR at pH 3.0 and 25 °C. The adsorption kinetics of the three dyes followed the pseudo-second-order model. In the multicomponent system, preferential adsorption was observed for AR at low adsorbent quantities due to the small size of the molecule. When the adsorbent amount was greater, AR1 was adsorbed first because of the greater number of sulfonic acid roots. In the entire adsorption process, XO always adsorbed most slowly.

Key words | acid dyes, competitive adsorption, magnetic quaternary chitosan salt, multicomponent

Conglu Zhang
Xiaomin Hu (corresponding author)
Institute of Resources and Civil Engineering,
Northeastern University,
Shenyang 110014,
China
E-mail: *hxmin_jj@163.com*

Conglu Zhang
Xiaohong Hou
Ning Liang
Yueyue Ding
School of Pharmaceutical Engineering,
Shenyang Pharmaceutical University,
Shenyang 110016,
China

INTRODUCTION

Acid dyes, which are typical dyes for use in an acidic medium, include azo dyes, anthraquinone dyes and triphenylmethane dyes. Like other organic dyes, they exhibit strong chemical stability, carcinogenesis, teratogenesis and mutagenesis (Luo *et al.* 2011). Thus, dye wastewater has become an important factor threatening the water environment (Ren *et al.* 2012). At present, the treatment methods for dye wastewater include the adsorption method (Ioannou *et al.* 2013), the electrochemical oxidation-reduction method (Zhou *et al.* 2011), advanced oxidation technology (Yuan *et al.* 2012) and the microbial-degradation method (Kolekar *et al.* 2012). However, adsorption has been recognised as a practical technology because of its high efficiency, simple operation and low energy consumption (Konicki *et al.* 2013).

In the literature on dye adsorption, numerous studies have mainly considered single-component adsorption (Shen *et al.* 2011; Auta & Hameed 2013; Rahman *et al.* 2013), and studies of mixed components are limited (Wang *et al.* 2012; Kumar & Tamilarasan 2013). In fact, competitive adsorption usually occurs in multicomponent systems, which may be attributed to the adsorption of different components onto the same type of active centre. In addition, the degree of adsorption of each component depends on its chemical and physical properties, the force between each component and the active centre. In reality, most dye wastewaters contain more than one dye. Therefore, it is important to study dye adsorption in multicomponent systems.

Chitosan is characterised as a remarkable biosorbent. As a result of the presence of hydroxyl and amine groups, chitosan can be chemically modified. Quaternarisation is a type of modification method that can enhance its adsorption to anionic substances. In our previous work, a magnetic quaternary chitosan salt was prepared. In this work, acid red 1 (AR1), xylenol orange (XO) and alizarin red (AR) were selected to investigate competitive adsorption in multicomponent systems.

MATERIALS AND METHODS

Materials

Magnetic quaternary chitosan (CS/EPTAC/Fe_3O_4) particles were synthesised and used as a new adsorbent. Acid red 1 ($C_{18}H_{13}N_3NaO_8S_2$, $\lambda_{max} = 505$ nm), xylenol orange ($C_{31}H_{28}N_2Na_4O_{13}S$, $\lambda_{max} = 436$ nm), and alizarin red ($C_{14}H_7NaO_7S{\cdot}H_2O$, $\lambda_{max} = 422$ nm) were purchased from Aladdin Reagent Co., Ltd (Shanghai, China). All other chemical reagents were A. R.-grade reagents.

doi: 10.2166/wst.2014.276

Preparation of the CS/EPTAC/Fe_3O_4

CS/EPTAC/Fe_3O_4 with a molar ratio of m (CS/EPTAC): m (Fe_3O_4) = 2:1 was prepared using the suspension cross-linking technique. Briefly, a quaternary chitosan salt (CS/EPTAC, substitution degree of 0.98) was obtained by the reaction of chitosan (deacylation degree of 94.68%) with 2,3-epoxypropyl trimethylammonium chloride (EPTAC). The Fe_3O_4 was prepared using coprecipitation (Zhu *et al.* 2012). Then, 0.2 g of CS/EPTAC was dissolved in 20 mL of distilled water, and a specified amount of Fe_3O_4 was added into this solution. After ultrasonic dispersion, 50 mL of liquid paraffin and 2.5 mL of Span80 were added, and the mixture was stirred for 30 min at 30 °C. Afterwards, 3.0 mL of 50% (V/V) glutaraldehyde was added as a cross-linker, and the mixture was continuously stirred for 2.5 h at 60 °C. Finally, the CS/EPTAC/Fe_3O_4 was purified by magnetic field separation, washed with petroleum ether, ethanol and distilled water in turn, and vacuum-dried at 40 °C. For comparison, magnetic chitosan (CS/Fe_3O_4) was prepared under identical conditions.

Effect of the pH

The effect of the solution's pH was investigated in a triangular flask at 25 °C. The initial pH was adjusted from 2.0 to 10.0 using HCl and NaOH aqueous solutions. Then, 0.02 g of adsorbent was dispersed in 50 mL of three dye solutions (50 mg L^{-1}), respectively. The solutions were oscillated in incubator shakers with a shaking speed of 150 rpm for 24 h. Finally, the adsorbent was separated using an external magnetic field. The dye concentration was analysed using a UV-Vis spectrophotometer (UV2000, Unico Co., Ltd, China).

Single-system adsorption experiments

A specific concentration range of XO, AR1 and AR solutions were prepared, then 0.02 g of CS/EPTAC/Fe_3O_4 was added into the series of solutions (pH = 3.0). Thus, the adsorption kinetics and adsorption isotherm were studied at 25 °C.

The equilibrium adsorption capacity (Q_e, mg g^{-1}) and the removal rate (R, %) were calculated according to Equations (1) and (2) (Kyzas *et al.* 2013):

$$Q_e = \frac{(C_0 - C_e)V}{m} \quad (1)$$

$$R = \frac{(C_0 - C_e)}{C_0} \times 100\% \quad (2)$$

where C_0 and C_e (mg L^{-1}) are the initial and equilibrium concentrations of the dye in the solution, respectively; V (ml) is the volume of the solution; and m (g) is the mass of adsorbent.

Competitive-adsorption experiments

The competitive-adsorption experiment was conducted as follows: 0.005–0.025 g of CS/EPTAC/Fe_3O_4 was added into a triangular flask with 50 mL of a mixed dye solution (pH = 3.0). The triangular flasks were oscillated for 24 h at 25 °C. After magnetic separation, the dye solution was investigated.

The multicomponent dye concentration determination method

The calculation of each component in the mixture was performed according to the multicomponent absorbance additive property; that is, the total absorbance of the mixture is equal to the sum of the absorbance of the components in the mixture (Kyzas *et al.* 2009). The formulas were as follows:

$$A\lambda_{1x,y,z} = \varepsilon\lambda_{1x}lC_x + \varepsilon\lambda_{1y}lC_y + \varepsilon\lambda_{1z}lC_y \quad (3)$$

$$A\lambda_{2x,y,z} = \varepsilon\lambda_{2x}lC_x + \varepsilon\lambda_{2y}lC_y + \varepsilon\lambda_{2z}lC_y \quad (4)$$

$$A\lambda_{3x,y,z} = \varepsilon\lambda_{3x}lC_x + \varepsilon\lambda_{3y}lC_y + \varepsilon\lambda_{3z}lC_y \quad (5)$$

where l is the path length (cm); $\epsilon\lambda_{1x}$, $\epsilon\lambda_{1y}$, $\epsilon\lambda_{1z}$, $\epsilon\lambda_{2x}$, $\epsilon\lambda_{2y}$, $\epsilon\lambda_{2y}$, $\epsilon\lambda_{2z}$, $\epsilon\lambda_{3x}$, $\epsilon\lambda_{3y}$ and $\epsilon\lambda_{3z}$ are the molar absorption coefficients of each pure component at various wavelengths; $A\lambda_{1x,y,z}$, $A\lambda_{2x,y,z}$ and $A\lambda_{3x,y,z}$ are the mixed absorbances at various wavelengths; and C_x, C_y and C_z are the concentrations of each component.

RESULTS AND DISCUSSION

Characterisation

The surface morphology of CS/EPTAC/Fe_3O_4 was analysed using scanning electron microscopy (SEM, SSX-550, Shimadzu, Japan). The sample was coated with a thin layer of gold. The SEM data for CS/EPTAC/Fe_3O_4 are presented in Figure 1. As seen, most of the magnetic particles,

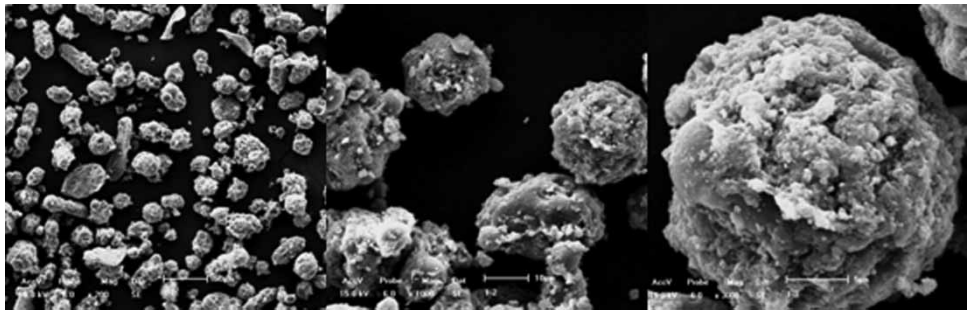

Figure 1 | SEM images of CS/EPTAC/Fe_3O_4.

with an average diameter of approximately 20 μm, were approximately spherical.

Effect of the pH on adsorption

Solution pH is the most important factor affecting the adsorption (Zhu *et al*. 2012). It can influence the adsorbent properties and the adsorbate chemical form. Figure 2 presents the results of adsorption by CS/EPTAC/Fe_3O_4 and CS/Fe_3O_4 for various pH values.

The results showed that the adsorption was higher under acidic conditions than under alkaline conditions for CS/EPTAC/Fe_3O_4 and CS/Fe_3O_4. The CS/EPTAC/Fe_3O_4 adsorption effect was superior to that of CS/Fe_3O_4 because the introduction of quaternary ammonium salt groups could improve the cationic strength of the chitosan. For CS/EPTAC/Fe_3O_4, the maximal removal was observed at pH 3.0. This was because the residual amine moieties in the chitosan would be protonated at a lower pH, behaving as extra adsorbent sites, which promoted adsorption. For pH < 3.0, the ionisation degree of the dye was weakened, and the adsorption was affected. Under alkaline conditions, the adsorption ability was limited, which may be due to the competition of OH^- with the anionic dye (Fan *et al*. 2012). In addition, under a magnetic field, the adsorbent was separated quickly. By weighing the adsorbent amounts before and after adsorption, it was not lost in the acidic media.

Adsorption isotherm

To study the adsorption mechanism and evaluate the adsorption properties of CS/EPTAC/Fe_3O_4, adsorption isotherms were studied. The results are shown in Figure 3.

Two important isotherm equations, namely the Langmuir (Equation (6)) and Freundlich (Equation (7)) isotherms (Zhang & Ou 2013), were selected for the adsorption study.

The Langmuir model is based on the assumption of a structurally homogeneous adsorbent and monolayer coverage with no interaction between the adsorbate molecules.

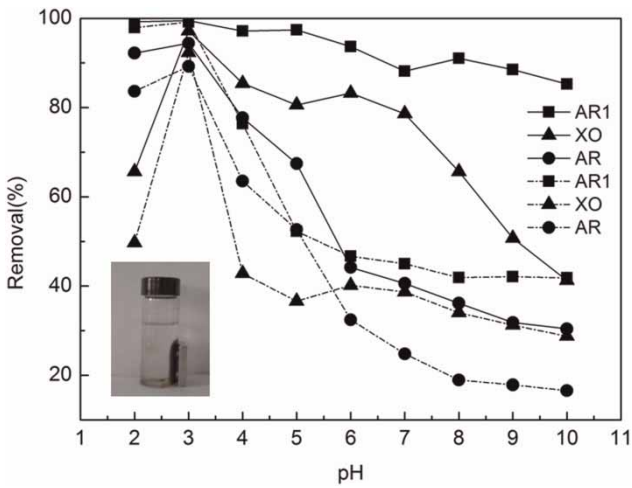

Figure 2 | Effect of pH on adsorption (solid line and dashed line represent CS/EPTAC/Fe_3O_4 and CS/Fe_3O_4, respectively).

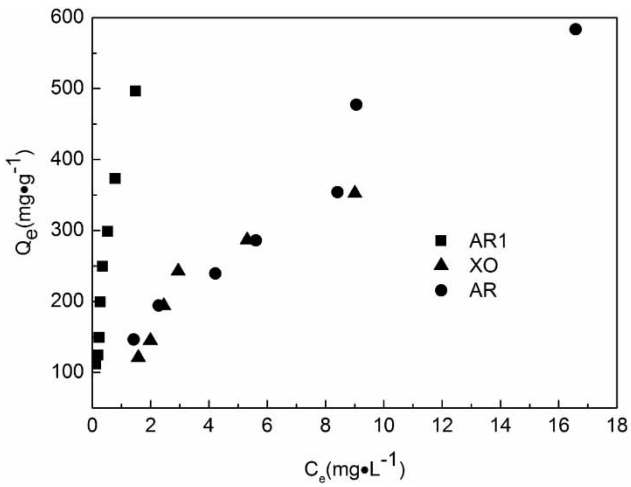

Figure 3 | Adsorption isotherms of the three dyes.

The equation is represented by

$$Q_e = \frac{Q_m K_L C_e}{1 + K_L C_e} \quad (6)$$

where Q_e is the equilibrium adsorption capacity of the dye on the adsorbent (mg g^{-1}); C_e is the equilibrium dye concentration in solution (mg L^{-1}); Q_m is the maximal capacity of the adsorbent (mg g^{-1}); and K_L is the Langmuir adsorption constant related to the free adsorption energy (L mg^{-1}).

The Freundlich model is based on the assumption that the adsorption occurs on heterogeneous surfaces with interaction between the adsorbed molecules. The Freundlich equation is

$$Q_e = KC_e^{1/n} \quad (7)$$

where K is the Freundlich adsorption constant that provides information about the extent of adsorption (L mg^{-1}); and n is the heterogeneity factor.

The model constants, along with the correlation coefficients, are listed in Table 1. Based on the results, the Langmuir constant K_L of AR1 exhibited a higher value (1.1753 L mg^{-1}) than those for XO (0.2197 L mg^{-1}) and AR (0.0832 L mg^{-1}), showing the higher affinity towards CS/EPTAC/Fe_3O_4. The maximum adsorption capacities were 781.55, 537.40 and 992.61 mg g^{-1} for AR1, XO and AR, respectively. The Freundlich constant K reached higher values, representing greater binding capacity between the adsorbent and adsorbate. In addition, the values of the constant n were 1.71, 1.92 and 1.67, respectively, which reflected the favourable adsorption of the dyes onto CS/EPTAC/Fe_3O_4.

Adsorption kinetics

The kinetic behaviour was studied at various initial dye concentrations. The adsorption approached the adsorption equilibrium within approximately 2 h, as shown in Figure 4. The three dyes showed rapid adsorption in the first 30 min and then decreased. This was mainly because many of the active sites on the adsorbent surfaces were not occupied at the beginning. When the concentration of the dye decreased gradually, the number of active sites was gradually reduced. Therefore, the adsorption rate decreased until adsorption equilibrium. In addition, an increase in the initial concentration of the dye extended the adsorption equilibrium time. This suggested that the dye concentration was also a factor influencing the adsorption rate.

To determine the characteristic constants of adsorption, a pseudo-first-order kinetics model (Equation (8)) and a pseudo-second-order kinetics model (Equation (9)) (Li *et al.* 2013) were used to fit the adsorption process. The linear forms of the two models are

$$\lg(Q_e - Q_t) = -\frac{K_1 t}{2.303} + 1gQ_e \quad (8)$$

$$\frac{t}{Q_T} = \frac{1}{Q_e} t + \frac{1}{K_2 Q_e^2} \quad (9)$$

where Q_t is the amount of dye adsorbed at a time t (mg g^{-1}), K_1(min^{-1}) and K_2(g mg^{-1} min^{-1}) are the adsorption rate constants of the pseudo-first-order and pseudo-second-order models, respectively, and t(min) is the time. The fitting results were presented in Table 2.

As indicated in Table 2, the correlation coefficients (R^2) of the pseudo-second-order model were higher than those for the pseudo-first-order model. Thus, the adsorption was dominated by chemical adsorption. In addition,

Table 1 | Fitting results of the adsorption isotherms

Adsorption isotherm		Dyes		
		AR1	XO	AR
Langmuir	Q_m	781.55	537.40	992.61
	K_L	1.1753	0.2197	0.0832
	R^2	0.9838	0.9451	0.9201
Freundlich	K	407.62	116.39	109.95
	n	1.7111	1.9230	1.6716
	R^2	0.9643	0.9040	0.9415

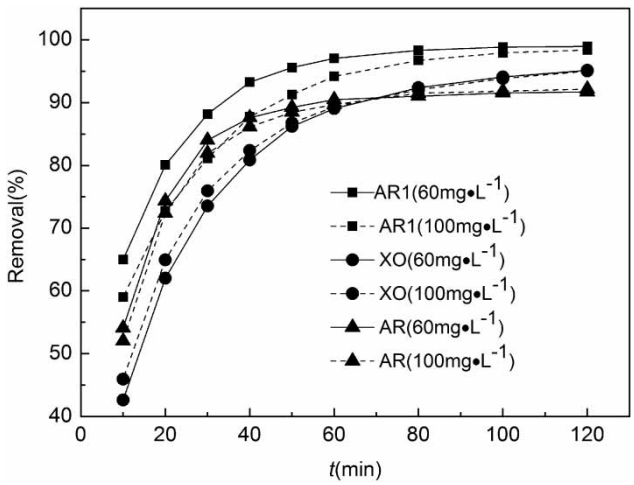

Figure 4 | Effects of the initial concentration.

Table 2 | Kinetic parameters of the first-order and second-order kinetic models

			First-order			Second-order		
Dye	C_0/mg L^{-1}	Q_e'/mg g^{-1}	$K_1\times10^3$/min^{-1}	Q_e/mg g^{-1}	R^2	$K_2\times10^3$/g mg^{-1} min^{-1}	Q_e/mg g^{-1}	R^2
AR1	60	149.41	36.85	50.11	0.9491	1.22	156.25	0.9996
	100	249.14	32.47	117.25	0.9815	0.46	263.16	0.9997
XO	60	145.72	29.94	87.44	0.9810	0.45	161.29	0.9990
	100	244.32	26.02	124.05	0.9654	0.33	263.16	0.9995
AR	60	146.45	16.81	38.45	0.7306	1.27	144.93	0.9988
	100	239.46	20.96	74.01	0.8344	0.62	243.90	0.9990

the adsorption rate constants (K_2) decreased gradually with increased dye concentration. This was mainly because the adsorption competition of the dye molecules was small at lower concentrations. In contrast, at higher concentrations, this competition was high, and consequently, the adsorption rate was decreased (Zhang *et al.* 2012).

Dye-adsorption studies in multicomponent systems

To analyse the combination of dyes and CS/EPTAC/Fe_3O_4 by comparing the dye adsorption amounts in the mixed system, the following equation was established:

$$\theta_1/\theta_2 = (C_{0l} - C_l)/(C_{02} - C_2) \tag{10}$$

where θ_1/θ_2 is the ratio of the adsorption amount of the two dyes. The larger the value, the greater the competition of the two dyes, where C_l and C_2 (mg L^{-1}) are the residual concentrations of the two dyes, respectively, and C_{01} and C_{02} (mg L^{-1}) are the initial concentrations of the two dyes, respectively.

The results of competitive adsorption are presented in Figure 5. In Figure 5(a), the AR1 concentration shows a

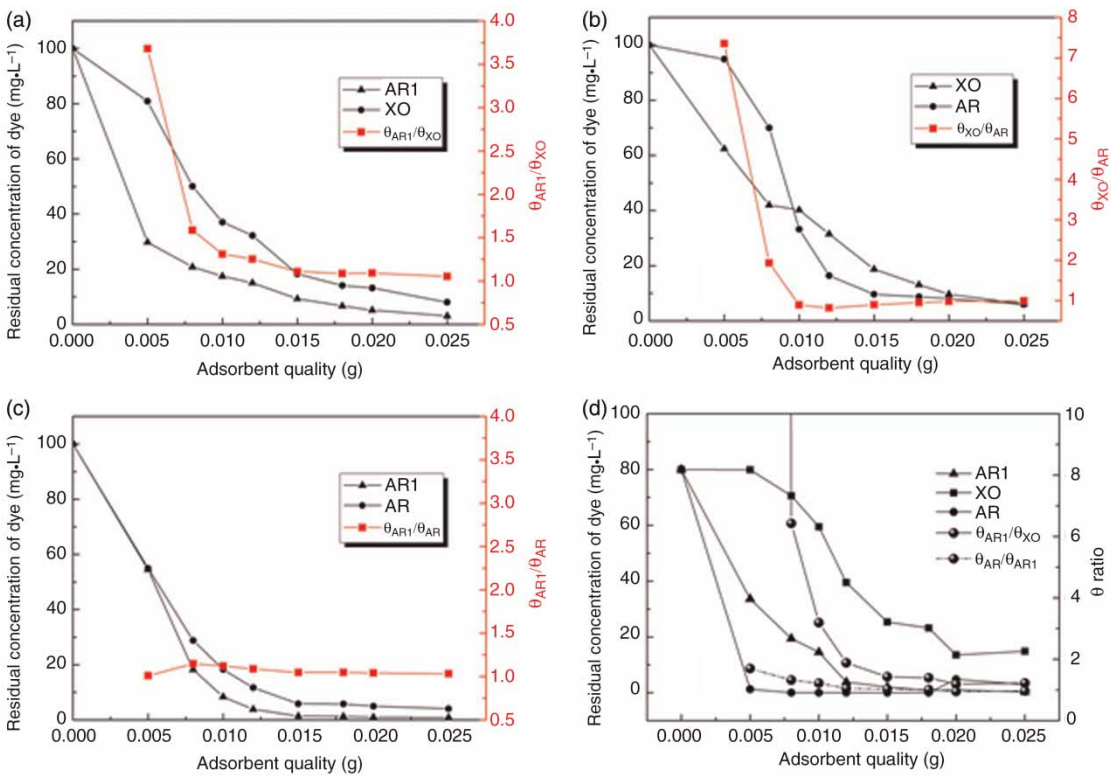

Figure 5 | Competitive adsorption in the multicomponent systems.

nearly linear decline with increased adsorbent amount. In comparison, the XO concentration declined slowly. This phenomenon showed that the interaction force between AR1 and CS/EPTAC/Fe_3O_4 was stronger than the force between XO and CS/EPTAC/Fe_3O_4. However, it is worth noting that the two dye concentrations had identical downward trends for adsorbent amounts greater than 0.015 g, and the θ_{AR1}/θ_{xo} ratio began approaching 1. The dissimilar adsorption could be due to the different molecular structures and characteristics of the dyes. AR1 has two sulfonic acid roots, and XO has a sulfonic acid root and four carboxylic acid roots. The three-dimensional structure of AR1 is smaller than that of XO. Therefore, AR1 may be more easily adsorbed.

Figure 5(b) shows that when the adsorbent amount was less than 0.01 g, the adsorption amount of AR was less than that of XO. This could be attributed to the difference in the functional groups in the dyes. That is, there are four carboxylic acid roots in XO, and there is one sulfonic acid root in AR. The combination of the dyes and CS/EPTAC/Fe_3O_4 was mainly achieved by the role of positive and negative charges. Thus, at low adsorbent amounts, the charge attraction between XO and the adsorbent was much stronger. When the amount exceeded 0.01 g, because of the large three-dimensional structure, XO instead became more difficult to adsorb.

Figure 5(c) showed that, within the scope of the experiment, the θ_{AR1}/θ_{AR} value always stayed near 1, which may be due to the differing number of sulfonic acid roots in the dyes and the different three-dimensional structure. AR1 has two sulfonic acid roots and is a larger molecule. In contrast, AR has one sulfonic acid root and is a smaller molecule. Thus, in competitive adsorption, the advantages of the respective dyes were not obvious.

In the ternary system, the three dyes showed obvious differences in the decolourising order presented in Figure 5(d). When the adsorbent amount was less than 0.018 g, the order of the combined amount of dye was AR > AR1 > XO, but the difference between AR1 and AR was small. It is worth noting that AR exhibited desorption and the combined amount of AR1 increased slightly when the adsorbent amount exceeded 0.018 g. Due to the high dye concentration, the dye-molecule spatial effect became a main influencing factor. Thus, when the adsorbent amount was small, AR1 mainly competed with AR, and the micromolecular AR molecule was preferentially adsorbed. When the adsorbent quantity was large, AR1 was adsorbed first because of the two sulfonic acid roots. Throughout the entire process, XO always exhibited the slowest adsorption.

CONCLUSIONS

(1) The adsorption processes of CS/EPTAC/Fe_3O_4 and the three dyes (AR1, XO and AR) occurred mainly via electrostatic interactions. Thus, the optimal adsorption effect appeared at pH = 3.0.
(2) In the single system, the CS/EPTAC/Fe_3O_4 was very effective for the removal of the three dyes. The maximal dye-adsorption capacities of CS/EPTAC/Fe_3O_4 were 781.55, 537.40 and 992.61 mg g^{-1} for AR1, XO and AR, respectively, and the adsorption kinetics of the three dyes followed the pseudo-second-order model.
(3) In multicomponent systems, preferential adsorption was observed for AR because the molecules are small at low adsorbent quantities. For a large adsorbent amount, AR1 was adsorbed first because of the greater number of sulfonic acid roots. Throughout the entire adsorption process, XO always exhibited the slowest adsorption.

ACKNOWLEDGEMENT

This study was supported by the National Natural Science Foundation of China (No. 51178088).

REFERENCES

Auta, M. & Hameed, B. H. 2013 Coalesced chitosan activated carbon composite for batch and fixed-bed adsorption of cationic and anionic dyes. *Colloids and Surfaces B: Biointerfaces* **105**, 199–206.

Fan, L. L., Zhang, Y., Li, X. J., Luo, C. N., Lu, F. G. & Qiu, H. M. 2012 Removal of alizarin red from water environment using magnetic chitosan with Alizarin Red as imprinted molecules. *Colloids and Surfaces B: Biointerfaces* **91**, 250–257.

Ioannou, Z., Karasavvidis, Ch., Dimirkou, A. & Antoniadis, V. 2013 Adsorption of methylene blue and methyl red dyes from aqueous solutions onto modified zeolites. *Water Science and Technology* **67** (5), 1129–1136.

Kolekar, Y. M., Nemade, H. N., Markad, V. L., Adav, S. S., Patole, M. S. & Kodam, K. M. 2012 Decolorization and biodegradation of azo dye, reactive blue 59 by aerobic granules. *Bioresource Technology* **104**, 818–822.

Konicki, W., Sibera, D., Mijowska, E., Lendzion-Bielun, Z. & Narkiewicz, U. 2013 Equilibrium and kinetic studies on acid dye Acid Red 88 adsorption by magnetic $ZnFe_2O_4$ spinel ferrite nanoparticles. *Journal of Colloid and Interface Science* **398**, 152–160.

Kumar, M. & Tamilarasan, R. 2013 Modeling studies: adsorption of aniline blue by using Prosopis Juliflora carbon/Ca/alginate

polymer composite beads. *Carbohydrate Polymers* **92**, 2171–2180.

Kyzas, G. Z., Bikiaris, D. N. & Lazaridis, N. K. 2009 Selective separation of basic and reactive dyes by molecularly imprinted polymers (MIPs). *Chemical Engineering Journal* **149**, 263–272.

Kyzas, G. Z., Lazaridis, N. K. & Bikiaris, D. N. 2013 Optimization of chitosan and β-cyclodextrin molecularly imprinted polymer synthesis for dye adsorption. *Carbohydrate Polymers* **91**, 198–208.

Li, Y. H., Du, Q. J., Liu, T. H., Peng, X. J., Wang, J. J., Sun, J. K., Wang, Y. H., Wu, S. L., Wang, Z. H., Xia, Y. Z. & Xia, L. H. 2013 Comparative study of methylene blue dye adsorption onto activated carbon, graphene oxide, and carbon nanotubes. *Chemical Engineering Research and Design* **91**, 361–368.

Luo, X. B., Zhan, Y. C., Huang, Y. N., Yang, L. X., Tu, X. M. & Luo, S. L. 2011 Removal of water-soluble acid dyes from water environment using a novel magnetic molecularly imprinted polymer. *Journal of Hazardous Materials* **187**, 274–282.

Rahman, A., Urabe, T. & Kishimoto, N. 2013 Color removal of reactive procion dyes by clay adsorbents. *Procedia Environmental Sciences* **17**, 270–278.

Ren, N. Q., Zhou, X. J., Guo, W. Q. & Yang, S. S. 2012 A review on treatment methods of dye wastewater. *CIESC Journal* **64**, 84–94.

Shen, C. S., Shen, Y., Wen, Y. Z., Wang, H. Y. & Liu, W. P. 2011 Fast and highly efficient removal of dyes under alkaline conditions using magnetic chitosan-Fe (III) hydrogel. *Water Research* **45**, 5200–5210.

Wang, S. B., Ng, C. W., Wang, W. T., Li, Q. & Hao, Z. P. 2012 Synergistic and competitive adsorption of organic dyes on multiwalled carbon nanotubes. *Chemical Engineering Journal* **197**, 34–40.

Yuan, R. X., Ramjaun, S. N., Wang, Z. H. & Liu, J. S. 2012 Photocatalytic degradation and chlorination of azo dye in saline wastewater: kinetics and AOX formation. *Chemical Engineering Journal* **192**, 171–178.

Zhang, J. X. & Ou, L. L. 2013 Kinetic, isotherm and thermodynamic studies of the adsorption of crystal violet by activated carbon from peanut shells. *Water Science and Technology* **67** (4), 737–744.

Zhang, J. X., Zhou, Q. X. & Ou, L. L. 2012 Kinetic, isotherm, and thermodynamic studies of the adsorption of methyl orange from aqueous solution by chitosan/alumina composite. *Journal of Chemical & Engineering Data* **57**, 412–419.

Zhou, M., Sarkka, H. & Sillanpaa, M. 2011 A comparative experimental study on methyl orange degradation by electrochemical oxidation on BDD and MMO electrodes. *Separation and Purification Technology* **78**, 290–297.

Zhu, H. Y., Fu, Y. Q., Jiang, R., Yao, J., Xiao, L. & Zeng, G. M. 2012 Novel magnetic chitosan/poly (vinyl alcohol) hydrogel beads: preparation, characterization and application for adsorption of dye from aqueous solution. *Bioresource Technology* **105**, 24–30.

First received 13 March 2014; accepted in revised form 30 May 2014. Available online 17 June 2014